Exploration of Functional Group Effects on D_2/H_2 Separation Selectivity within the UiO-66 Framework

Xiufang Li[a], Yanxi Tan[a,b], Zhanfeng Ju[b], Wenjing Wang[a,b,*], and Daqiang Yuan[a,b,*]

a University of the Chinese Academy of Sciences, Beijing 100049, China

b State Key Laboratory of Structural Chemistry, Fujian Institute of Research on the Structure of Matter, Chinese Academy of Sciences, Fuzhou 350002, China

*Email: wjwang@fjirsm.ac.cn or ydq@fjirsm.ac.cn

General procedures

Gas adsorption isotherms

Prior to gas adsorption testing, **UiO-66** and its derivatives were soaked in MeOH for solvent exchange for three days to remove the high-boiling solvent. Then, these samples were soaked in CH_2Cl_2 for another three days. Subsequently, approximately 100-150 mg of sample was activated at 100 °C for 24 h under dynamic vacuum (≤ 10 μm Hg). Adsorption and desorption experiments of H_2, D_2 and N_2 were performed using a Micromeritics ASAP 2020 PLUS instrument equipped with commercial software for data calculation and analysis at different temperatures. The test temperatures were controlled by soaking sample cell into liquid nitrogen bath (77 K) or liquid argon bath (87 K).

The isosteric enthalpy of adsorption is calculated from single-component gas equilibrium adsorption isotherms at different temperatures according to the Virial Method:

$$\ln(P) = \ln(N) + \left(\frac{1}{T}\right)\sum_{i=0}^{m} a_i \times N^i + \sum_{j=0}^{n} b_j \times N^j$$

where, P is the pressure in mmHg, N is the amount adsorbed in mg/g, T is the temperature in K, a_i and b_j represents virial coefficients, and m and n specify the number of coefficients needed for a precise description of the isotherms. The values of the virial coefficients a_0 to a_m were further used to determine the isosteric enthalpy of adsorption according to the following equation:

$$Q_{st} = -R \times \sum_{i=0}^{m} a_i \times N^i$$

where Q_{st} is the coverage-dependent isosteric enthalpy of adsorption in kJ/mol and R is universal gas constant with the value of 8.314 J mol^{-1} K^{-1}.

Breakthrough Measurements

The complete breakthrough of D_2 was determined using downstream gas composition reaching that of feed gas. Based on the mass balance, the gas adsorption capacities can be attained from the following equation:

$$q_i = \frac{C_i V}{22.4} \times \int_0^t \left(1 - \frac{F}{F_0}\right) dt$$

Where q_i refers to the equilibrium adsorption capacity of gas i (mmol g^{-1}), C_i represents the feed gas concentration, V refers to the volumetric feed flow rate (cm^3 min^{-1}), t represents the adsorption time (min), F_0 and F, respectively, refer to the inlet and outlet gas molar flow rates, and m represents adsorbent mass of (g). The separation factor (α) of breakthrough experiment can be calculated as follows:

$$\alpha = \frac{q_A y_B}{q_B y_A}$$

In which y_i is molar fraction of gas i ($i = A,B$) in gas mixture.

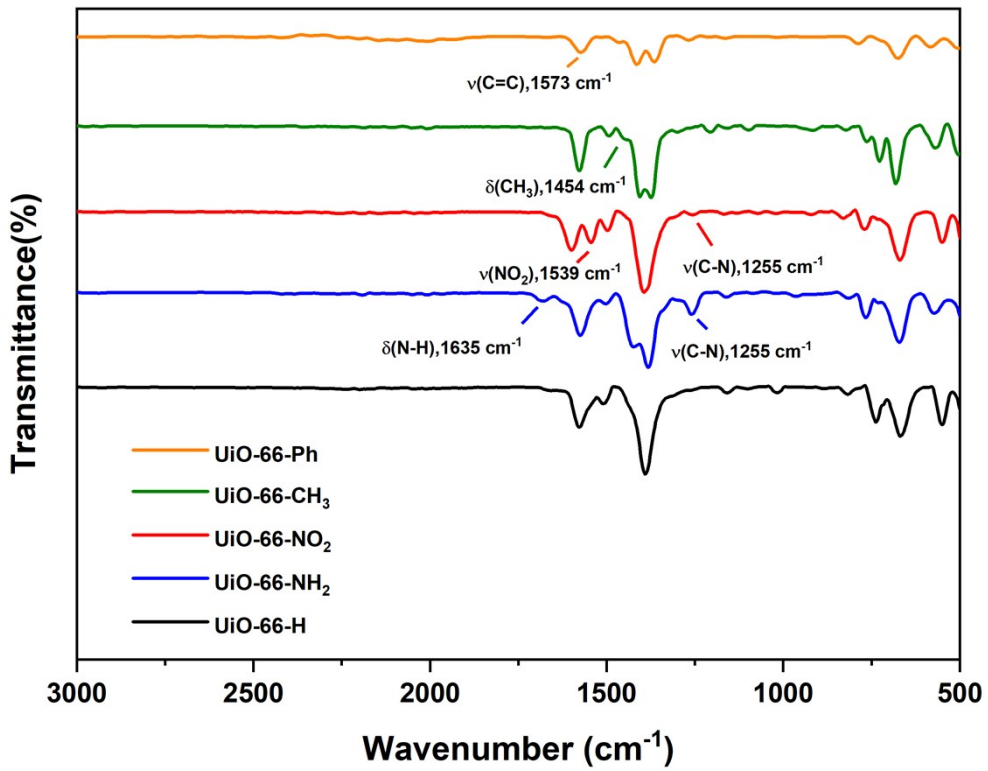

Fig. S1 IR spectra of **UiO-66** and its derivatives.

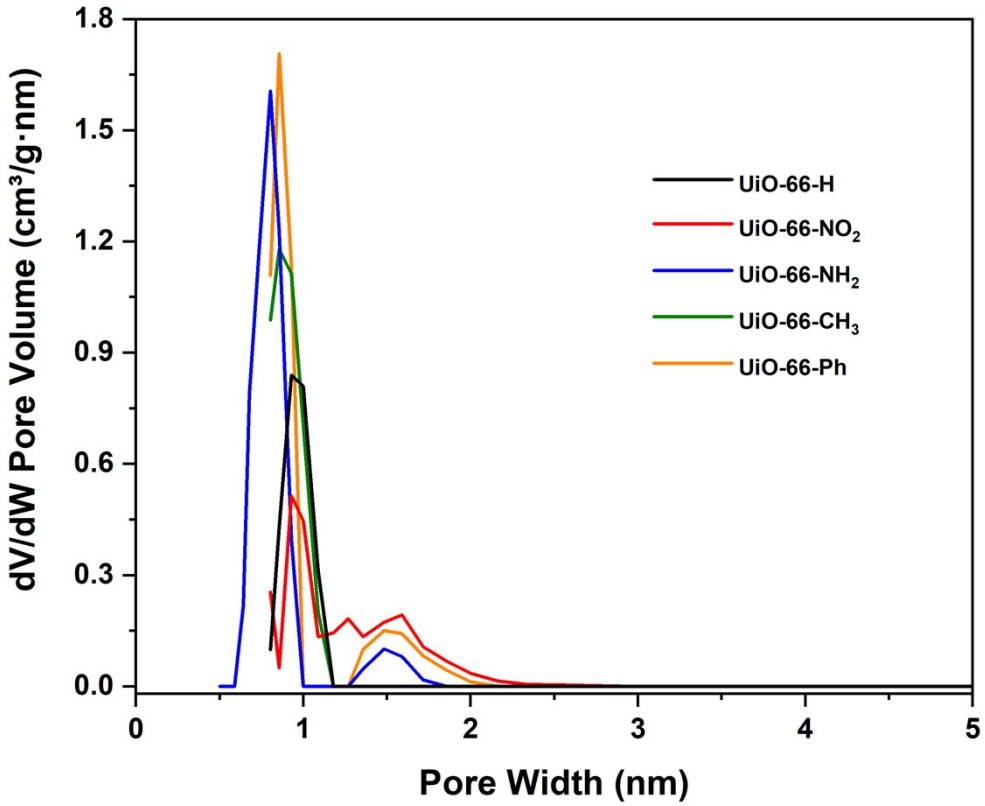

Fig. S2 Pore size distributions for **UiO-66** and its derivatives by using DFT method.

Table S1 Surface area, hydrogen isotopes uptake and micropore volume for **UiO-66** and its derivatives

	UiO-66	**UiO-66-NH_2**	**UiO-66-NO_2**	**UiO-66-CH_3**	**UiO-66-Ph**
BET (m^2/g)	1257	1017	974	909	890
77 K H_2 (mol/mol)	62.8	63.0	59.0	60.1	53.5
77 K D_2 (mol/mol)	69.2	68.4	64.2	67.5	57.9
87 K H_2 (mol/mol)	44.8	50.3	44.6	48.9	42.2
87 K D_2 (mol/mol)	48.6	53.9	49.0	51.1	45.6
Micropore volume (cm^3/g)	0.483	0.388	0.435	0.360	0.325

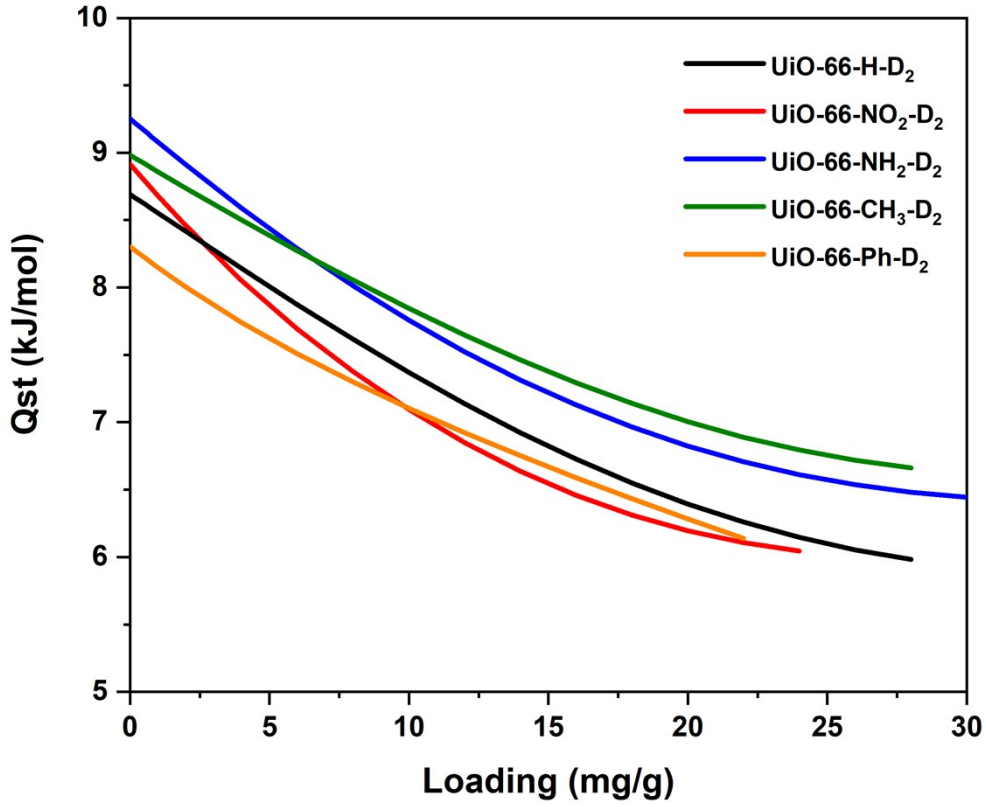

Fig. S3 Q_{st} values of D_2 for **UiO-66** and its derivatives.

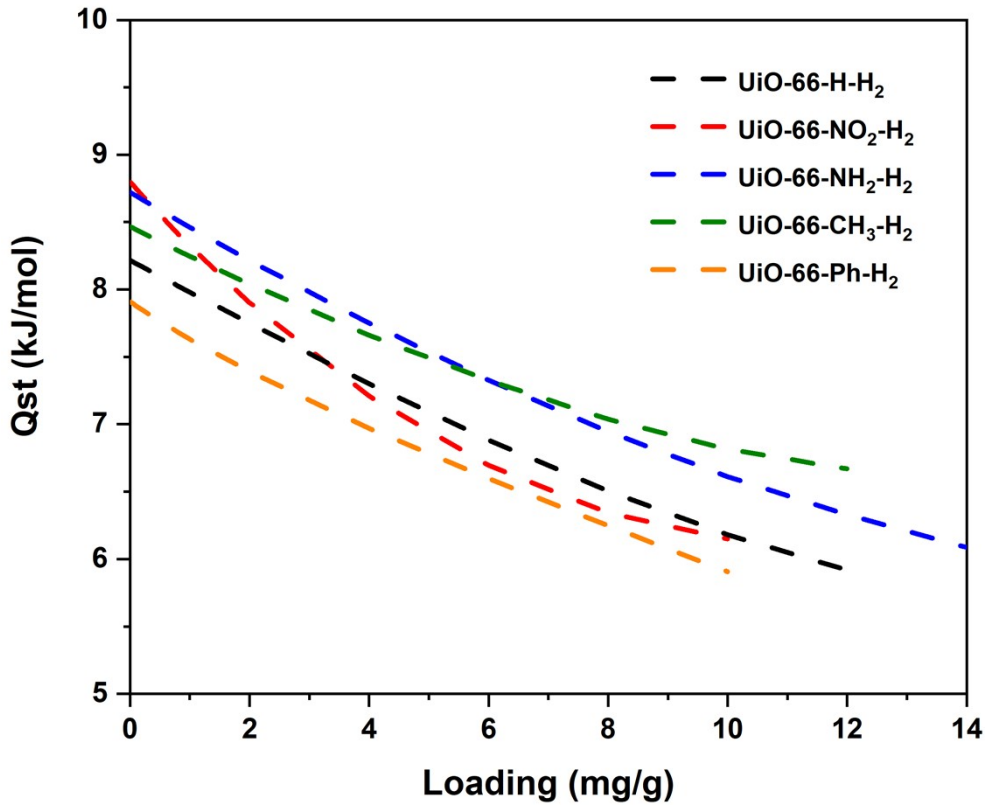

Fig. S4 Q_{st} values of H_2 for **UiO-66** and its derivatives.

(a)

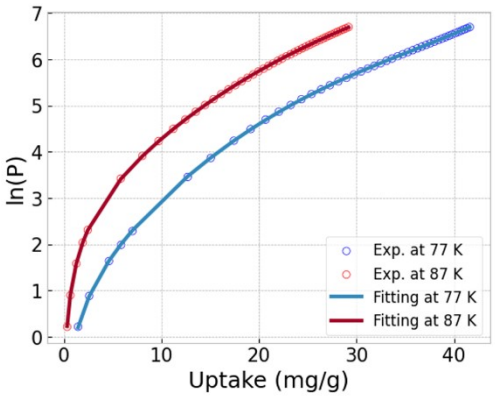

(b)

	Parameter Value	Standard Deviation
a_0	-1.045328e+03	4.738792e+00
a_1	1.655738e+01	7.004006e-01
a_2	3.559111e-02	3.834810e-02
a_3	-1.151567e-02	2.082269e-03
a_4	1.492652e-04	5.393693e-05
a_5	-2.756261e-07	5.033719e-07
b_0	1.327436e+01	5.534581e-02
b_1	-1.385130e-01	7.674057e-03
b_2	2.713397e-03	2.329249e-04
Adj.r_squared	0.99999	

Fig. S5 (a)Virial equation fitting of D_2 adsorption isotherm of **UiO-66** at 77 K and 87 K. (b)Relevant fitting parameters for D_2.

(a)

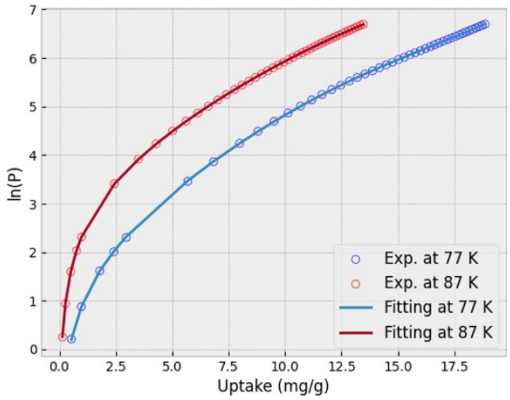

(b)

	Parameter Value	Standard Deviation
a_0	-9.882550e+02	4.077128e+00
a_1	2.871482e+01	1.335435e+00
a_2	-2.905582e-01	1.655464e-01
a_3	9.709325e-03	2.031113e-02
a_4	2.031113e-02	2.031113e-02
a_5	1.062401e-04	2.396133e-05
b_0	1.357887e+01	4.788616e-02
b_1	-2.211570e-01	1.473933e-02
b_2	8.074862e-03	9.837410e-04
Adj.r_squared	0.99999	

Fig. S6 (a)Virial equation fitting of H_2 adsorption isotherm of **UiO-66** at 77 K and 87 K. (b)Relevant fitting parameters for H_2.

(a)

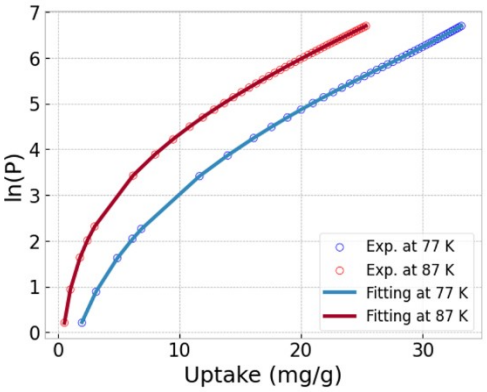

(b)

	Parameter Value	Standard Deviation
a_0	-1.072487e+03	2.899492e+00
a_1	2.931302e+01	4.891075e-01
a_2	-9.025968e-01	3.606648e-02
a_3	2.146209e-02	2.419862e-03
a_4	-5.691658e-04	7.609513e-05
a_5	6.764886e-06	8.683065e-07
b_0	1.308992e+01	3.326329e-02
b_1	-1.736808e-01	5.074434e-03
b_2	4.828287e-03	1.708937e-04
Adj.r_squared	0.99999	

Fig. S7 (a)Virial equation fitting of D_2 adsorption isotherm of **UiO-66-NO_2** at 77 K and 87 K. (b)Relevant fitting parameters for D_2.

(a)

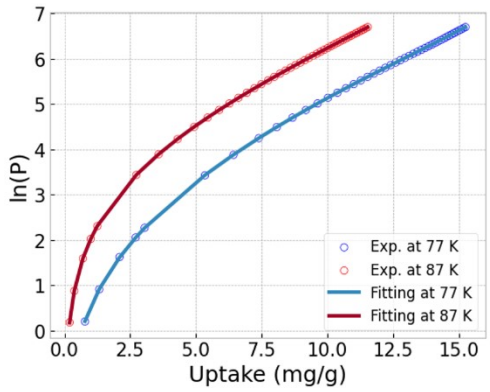

(b)

	Parameter Value	Standard Deviation
a_0	-1.058491e+03	2.311292e+00
a_1	6.108177e+01	8.593690e-01
a_2	-3.813825e+00	1.366653e-01
a_3	1.587380e-01	2.022040e-02
a_4	-9.245952e-03	1.394482e-03
a_5	2.322234e-04	3.480840e-05
b_0	1.392368e+01	2.663806e-02
b_1	-4.222818e-01	9.034307e-03
b_2	2.731370e-02	6.740710e-04
Adj.r_squared	0.99999	

Fig. S8 (a)Virial equation fitting of H_2 adsorption isotherm of **UiO-66-NO_2** at 77 K and 87 K. (b)Relevant fitting parameters for H_2.

(a)

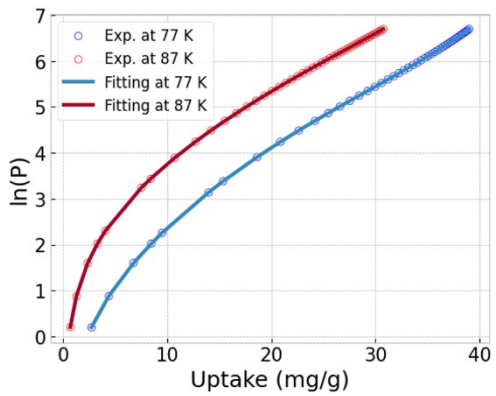

(b)

	Parameter Value	Standard Deviation
a_0	-1.112930e+03	1.337363e+00
a_1	2.126991e+01	1.843519e-01
a_2	-3.236897e-01	1.150401e-02
a_3	2.501602e-04	6.371660e-04
a_4	-6.961676e-05	1.691516e-05
a_5	1.679845e-06	1.633872e-07
b_0	1.331245e+01	1.529448e-02
b_1	-1.502539e-01	1.877826e-03
b_2	3.672020e-03	5.071206e-05
Adj.r_squared	0.99999	

Fig. S9 (a)Virial equation fitting of D_2 adsorption isotherm of **UiO-66-NH$_2$** at 77 K and 87 K. (b)Relevant fitting parameters for D_2.

(a)

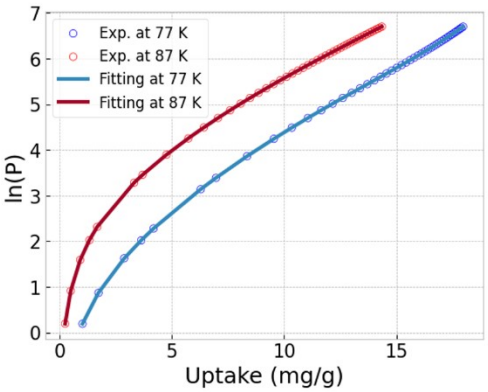

(b)

	Parameter Value	Standard Deviation
a_0	-1.049039e+03	1.324519e+00
a_1	3.202629e+01	4.002394e-01
a_2	-8.464218e-01	5.571483e-02
a_3	5.337618e-02	6.803857e-03
a_4	-5.047177e-03	3.940572e-04
a_5	1.523343e-04	8.289304e-06
b_0	1.356089e+01	1.524077e-02
b_1	-1.938236e-01	4.102071e-03
b_2	7.854957e-03	2.415677e-04
Adj.r_squared	0.99999	

Fig. S10 (a)Virial equation fitting of H_2 adsorption isotherm of **UiO-66-NH$_2$** at 77 K and 87 K. (b)Relevant fitting parameters for H_2.

(a)

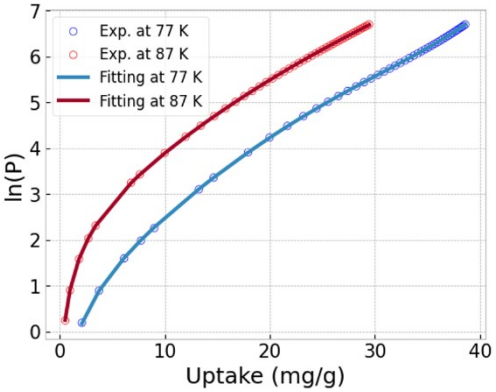

(b)

	Parameter Value	Standard Deviation
a_0	-1.080383e+03	4.822041e+00
a_1	1.502653e+01	6.878681e-01
a_2	-1.453398e-01	4.265834e-02
a_3	3.838016e-03	2.470783e-03
a_4	-3.165429e-04	6.713646e-05
a_5	4.806604e-06	6.608159e-07
b_0	1.327599e+01	5.565469e-02
b_1	-1.139251e-01	7.269950e-03
b_2	2.943440e-03	2.088492e-04
Adj.r_squared	0.99999	

Fig. S11 (a)Virial equation fitting of D_2 adsorption isotherm of **UiO-66-CH$_3$** at 77 K and 87 K. (b)Relevant fitting parameters for D_2.

(a)

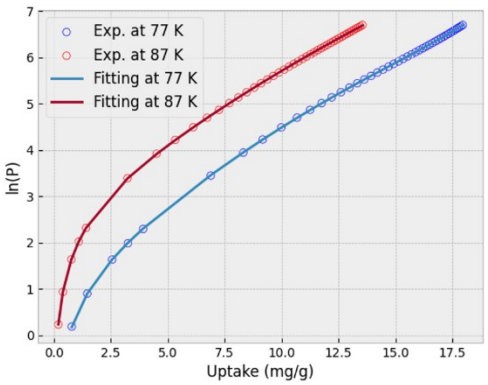

(b)

	Parameter Value	Standard Deviation
a_0	-1.018731e+03	4.301624e+00
a_1	2.793145e+01	1.357853e+00
a_2	-1.080983e+00	1.846144e-01
a_3	9.214833e-02	2.392399e-02
a_4	-8.645377e-03	1.403259e-03
a_5	2.296954e-04	2.970438e-05
b_0	1.350677e+01	4.979038e-02
b_1	-2.064536e-01	1.458054e-02
b_2	1.372811e-02	9.345533e-04
Adj.r_squared	0.99999	

Fig. S12 (a)Virial equation fitting of H_2 adsorption isotherm of **UiO-66-CH$_3$** at 77 K and 87 K. (b)Relevant fitting parameters for H_2.

(a)

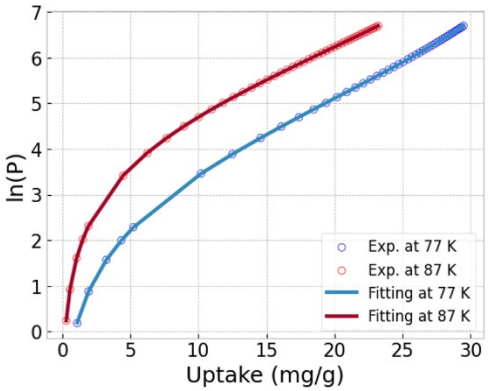

(b)

	Parameter Value	Standard Deviation
a_0	-9.989121e+02	2.118335e+00
a_1	1.963457e+01	4.154023e-01
a_2	-7.991885e-01	3.576619e-02
a_3	3.740059e-02	2.783547e-03
a_4	-1.073828e-03	9.968730e-05
a_5	1.334382e-05	1.288904e-06
b_0	1.290071e+01	2.462580e-02
b_1	-8.819437e-02	4.374929e-03
b_2	1.981143e-03	1.666985e-04
Adj.r_squared	0.99999	

Fig. S13 (a)Virial equation fitting of D_2 adsorption isotherm of **UiO-66-Ph** at 77 K and 87 K. (b)Relevant fitting parameters for D_2.

(a)

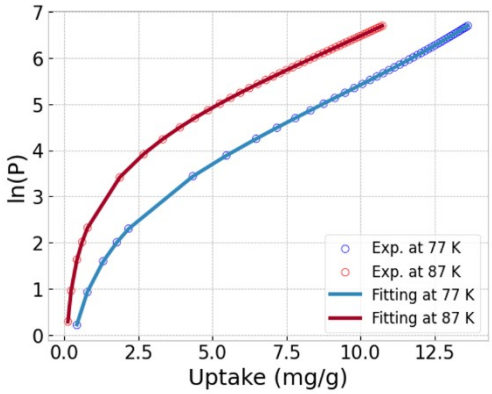

(b)

	Parameter Value	Standard Deviation
a_0	-9.513211e+02	2.053505e+00
a_1	3.587937e+01	8.833295e-01
a_2	-2.822027e+00	1.658553e-01
a_3	2.914122e-01	2.810670e-02
a_4	-1.727734e-02	2.187808e-03
a_5	4.577688e-04	6.142418e-05
b_0	1.331484e+01	2.400129e-02
b_1	-1.538242e-01	9.370036e-03
b_2	5.643399e-03	7.800525e-04
Adj.r_squared	0.99999	

Fig. S14 (a)Virial equation fitting of H_2 adsorption isotherm of **UiO-66-Ph** at 77 K and 87 K. (b)Relevant fitting parameters for H_2.

Table S2 Summary of experimentally measured hydrogen isotope separation performance on various porous materials

Compound	T_{exp} (K)	P_{exp} (kPa)	selectivity	Q_{st}-H_2 (kJ/mol)	Q_{st}-D_2 (kJ/mol)	Measurement methods	Ref.
UiO-66-H	77	100	1.31	8.21	8.69	Breakthrough	This work
UiO-66-NO_2			1.35	8.80	8.91		
UiO-66-NH_2			1.38	8.72	9.25		
UiO-66-CH_3			1.32	8.46	8.98		
UiO-66-Ph			1.34	7.91	8.30		
MOF-74-ac	25	1	7			TDS	1
	40		12				
	60		16				
	77		9				
MOF-74-IM-10	25		6				
	40		9				
	60		20				
	77		26				
FMOF-Cu	25	1	14			TDS	2
MFU-4l	50	1	1.7			TDS	3
Cu(I)-MFU-4l	100	1	11	32.7	35.0	TDS	4
CPO-27-Co	60	3	12	12.5	14.5	TDS	5
Ni_2Cl_2BBTA	77	1	4.5	6.0	6.7	TDS	6
MOF-303	25	100	21.6			TDS	7
Cu(I)Cu(II)-BTC	30	1	37.9	2.28	5.13	TDS	8
Ni_2(dobdc)	77	100	4.5	11.8	13.8	Breakthrough	9
Ni_2(dobpdc)			4.8	11	12.9		
Ni_2(olz)			5.6	11.8	12.9		
Ni_2(dotpdc)			4.6	11.1	12.6		
UTSC-700	30	1	7.3	3.5	4	TDS	10
FJI-Y9	77	100	1.3	6.0	6.2		11
FIR-29			1.2	5.8	6.1		
FJI-Y11	77	100	1.76	7.13	7.88	Breakthrough	12
Co(pyz)[$Pd(CN)_4$]	25	1	21.7	7.28	7.76	TDS	13
Cu-BDC-NH_2	77	100	1.6	7.03	7.14		14

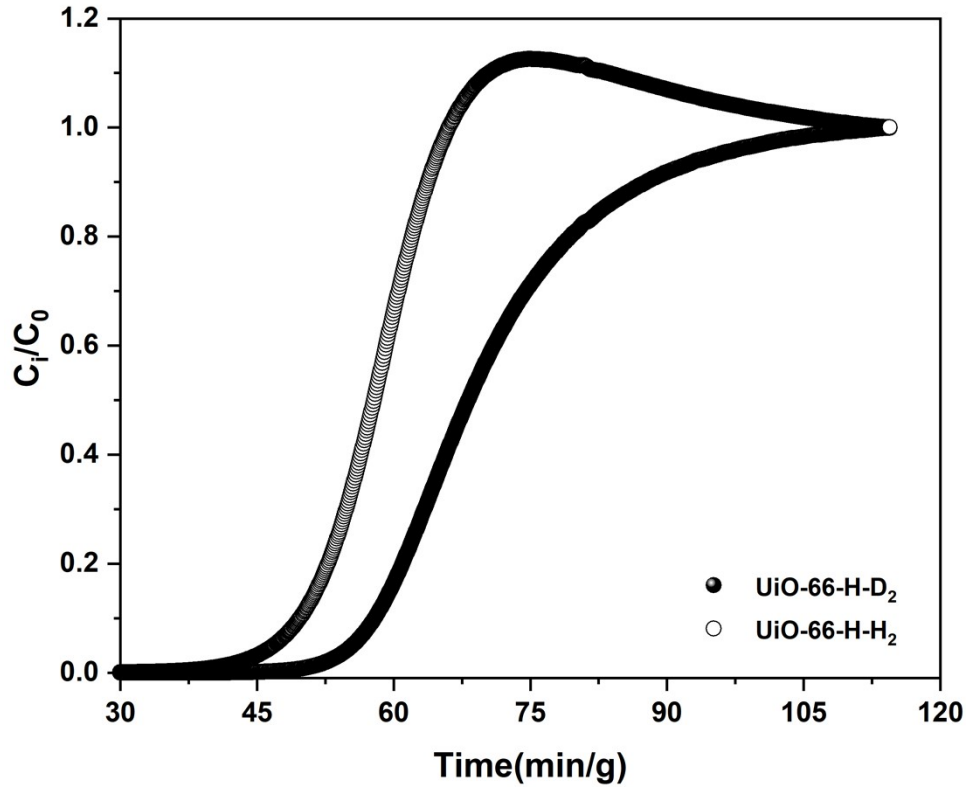

Fig. S15 Experimental breakthrough curves of **UiO-66** for the mixed gases of D_2/H_2/Ne (3/3/94, v/v) at 77 K and 1 bar.

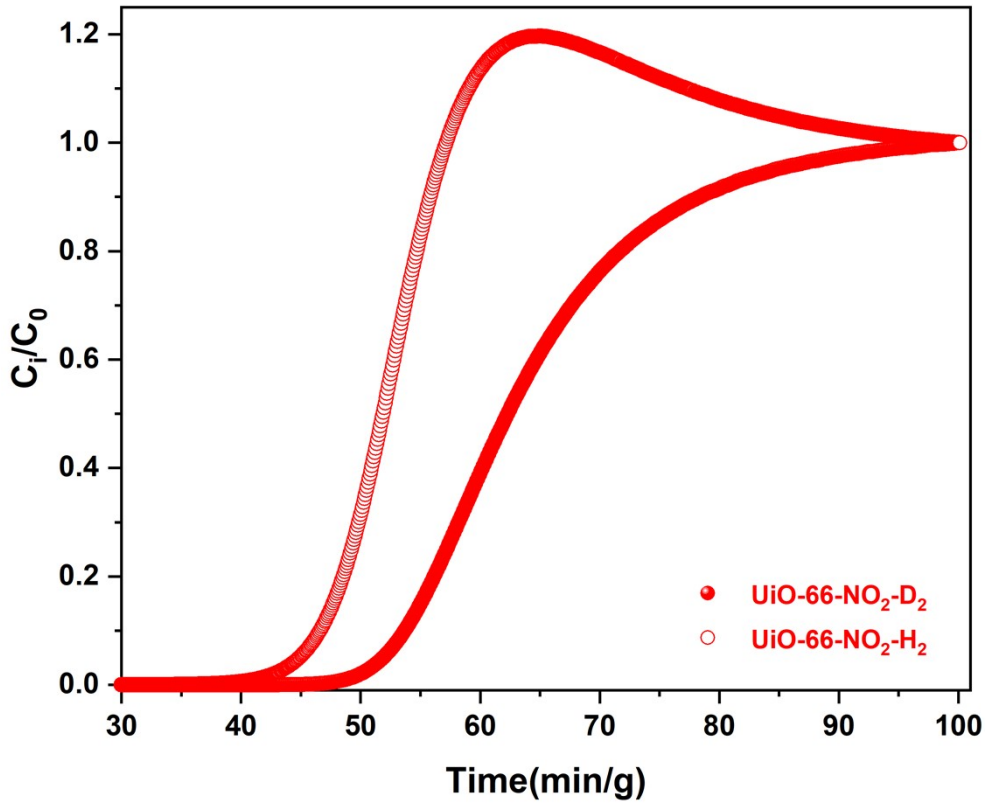

Fig. S16 Experimental breakthrough curves of **UiO-66-NO_2** for the mixed gases of D_2/H_2/Ne (3/3/94, v/v) at 77 K and 1 bar.

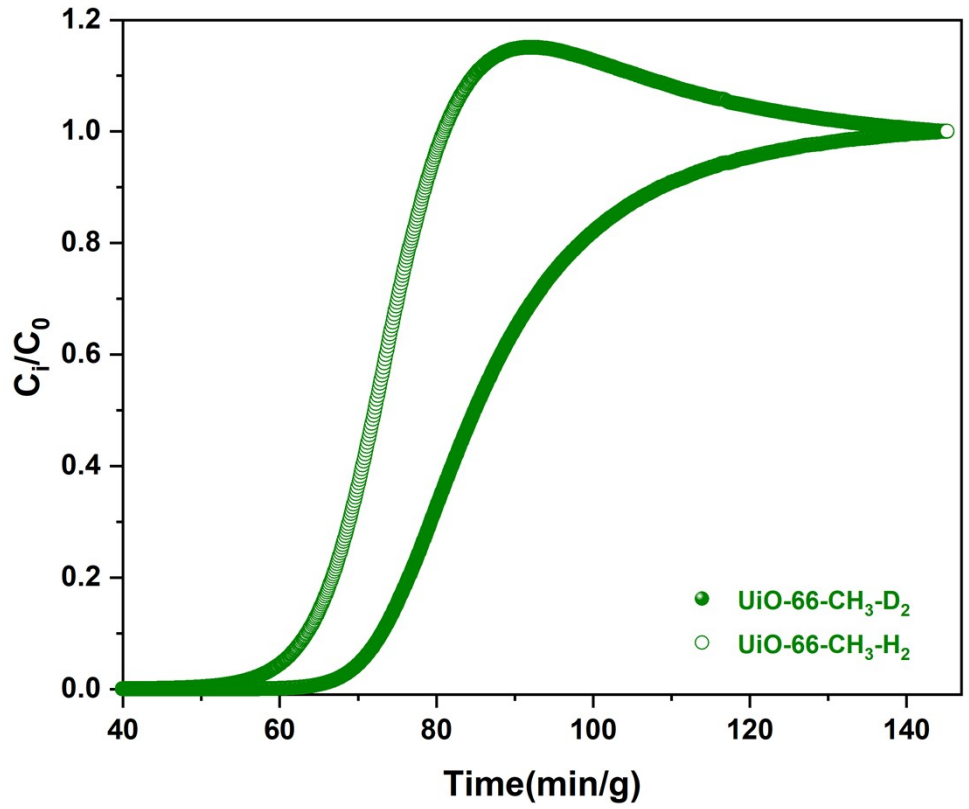

Fig. S17 Experimental breakthrough curves of **UiO-66-CH_3** for the mixed gases of D_2/H_2/Ne (3/3/94, v/v) at 77 K and 1 bar.

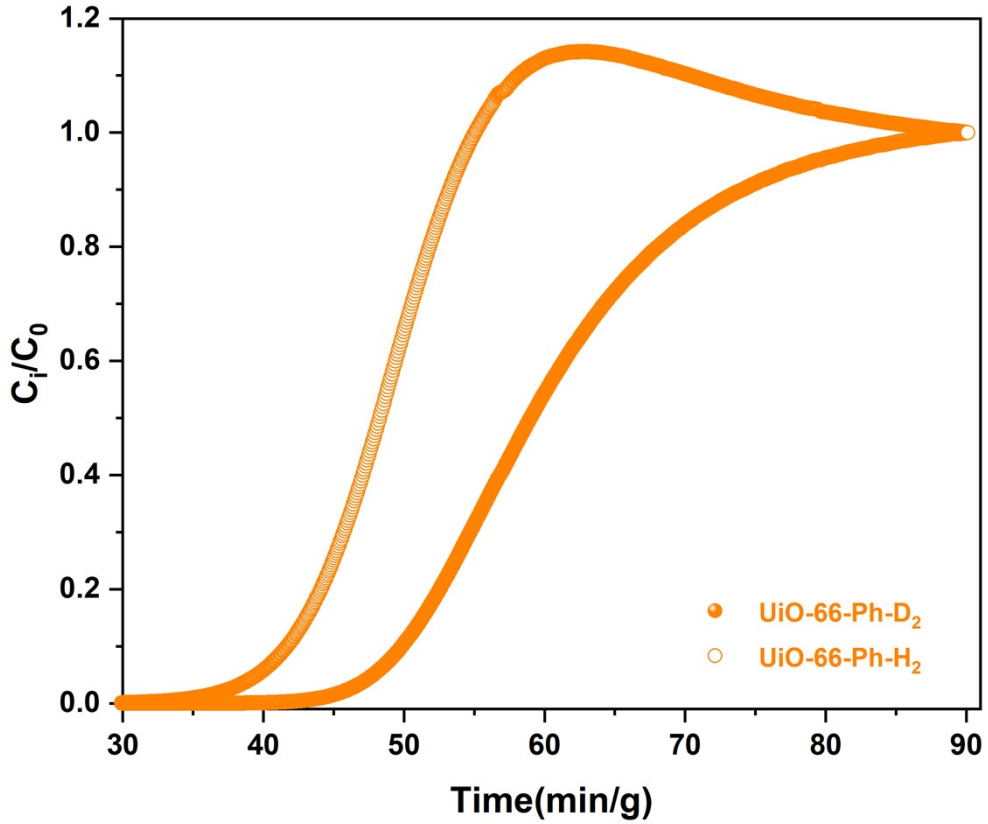

Fig. S18 Experimental breakthrough curves of **UiO-66-Ph** for the mixed gases of D_2/H_2/Ne (3/3/94, v/v) at 77 K and 1 bar.

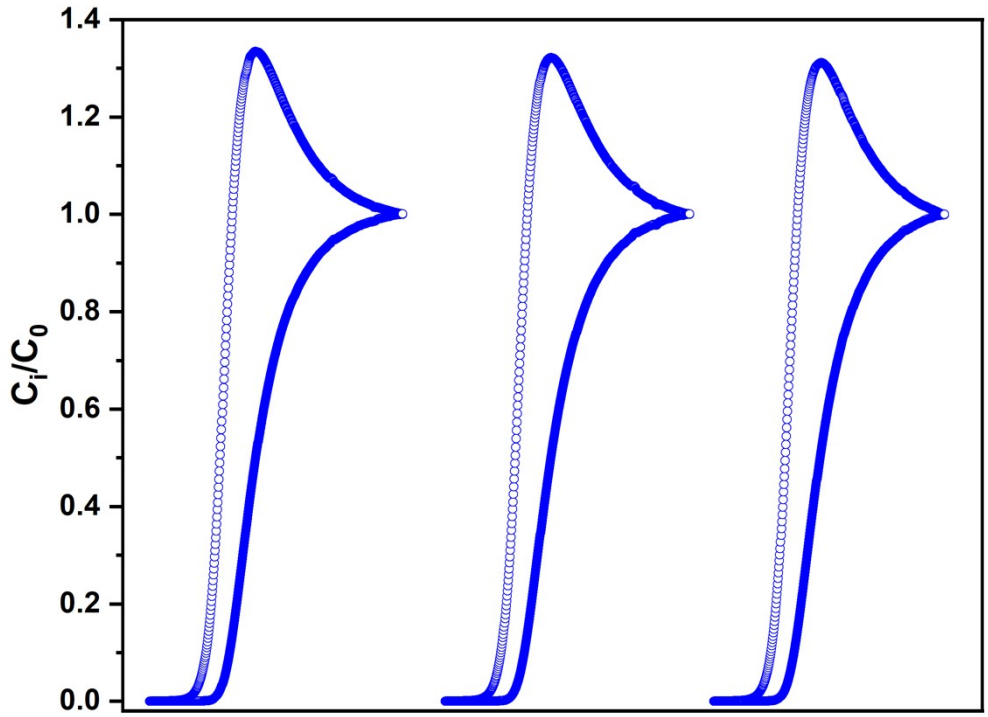

Fig. S19 Three consecutive breakthrough cycles of **UiO-66-NH$_2$** at 77 K.

References

1. J. Y. Kim, R. Balderas-Xicohtencatl, L. Zhang, S. G. Kang, M. Hirscher, H. Oh and H. R. Moon, Exploiting Diffusion Barrier and Chemical Affinity of Metal-Organic Frameworks for Efficient Hydrogen Isotope Separation, *J. Am. Chem. Soc.*, 2017, **139**, 15135-15141.
2. L. Zhang, S. Jee, J. Park, M. Jung, D. Wallacher, A. Franz, W. Lee, M. Yoon, K. Choi, M. Hirscher and H. Oh, Exploiting Dynamic Opening of Apertures in a Partially Fluorinated MOF for Enhancing H_2 Desorption Temperature and Isotope Separation, *J. Am. Chem. Soc.*, 2019, **141**, 19850-19858.
3. I. Savchenko, A. Mavrandonakis, T. Heine, H. Oh, J. Teufel and M. Hirscher, Hydrogen isotope separation in metal-organic frameworks: Kinetic or chemical affinity quantum-sieving?, *Micropor. Mesopor. Mat.*, 2015, **216**, 133-137.
4. I. Weinrauch, I. Savchenko, D. Denysenko, S. M. Souliou, H. H. Kim, M. Le Tacon, L. L. Daemen, Y. Cheng, A. Mavrandonakis, A. J. Ramirez-Cuesta, D. Volkmer, G. Schutz, M. Hirscher and T. Heine, Capture of heavy hydrogen isotopes in a metal-organic framework with active Cu(I) sites, *Nat. Commun.*, 2017, **8**, 14496.
5. H. Oh, I. Savchenko, A. Mavrandonakis, T. Heine and M. Hirscher, Highly Effective Hydrogen Isotope Separation in Nanoporous Metal–Organic Frameworks with Open Metal Sites: Direct Measurement and Theoretical Analysis, *ACS Nano*, 2014, **8**, 761-770.
6. X. Li, X. Wang, M. Li, J. Luo, Y. An, P. Li, J. Song, C. Chen, X. Feng and S. Wang, Highly selective adsorption of D_2 from hydrogen isotopes mixture in a robust metal bistriazolate framework with open metal sites, *Int. J. Hydrogen Energy*, 2020, **45**, 21547-21554.
7. H. Kim, S. Jee, J. Park, M. Jung, R. Muhammad, K. Choi and H. Oh, High D_2/H_2 selectivity performance in MOF-303 under ambient pressure for potential industrial applications, *Sep.*

Purif. Technol., 2023, **325**, 124660.

8. X. Hu, F. Ding, R. Xiong, Y. An, X. Feng, J. Song, L. Zhou, P. Li and C. Chen, Highly Effective H_2/D_2 Separation within the Stable Cu(I)Cu(II)-BTC: The Effect of Cu(I) Structure on Quantum Sieving, *ACS Appl. Mater. Interfaces*, 2023, **15**, 3941-3952.
9. L. Li, C. Ji, W. Wang, F. Wu, Y.-X. Tan and D. Yuan, The effect of pore sizes on D_2/H_2 separation conducted by MOF-74 analogues, *Inorg. Chem. Front.*, 2022, **9**, 1674-1680.
10. Q. Yan, J. Wang, L. Zhang, J. Liu, M. Wahiduzzaman, N. Yan, L. Yu, R. Dupuis, H. Wang, G. Maurin, M. Hirscher, P. Guo, S. Wang and J. Du, A squarate-pillared titanium oxide quantum sieve towards practical hydrogen isotope separation, *Nat. Commun.*, 2023, **14**, 4189.
11. F. J. Zhao, Y. X. Tan, W. Wang, Z. Ju and D. Yuan, Optimizing H_2, D_2, and C_2H_2 Sorption Properties by Tuning the Pore Apertures in Metal-Organic Frameworks, *Inorg. Chem.*, 2018, **57**, 13312-13317.
12. Y. Si, X. He, J. Jiang, Z. Duan, W. Wang and D. Yuan, Highly effective H_2/D_2 separation in a stable Cu-based metal-organic framework, *Nano Res.*, 2019, **14**, 518-525.
13. J. Ha, M. Jung, J. Park, H. Oh and H. R. Moon, Thermodynamic Separation of Hydrogen Isotopes Using Hofmann-Type Metal-Organic Frameworks with High-Density Open Metal Sites, *ACS Appl. Mater. Interfaces*, 2022, **14**, 30946-30951.
14. A. Dastbaz, J. Karimi-Sabet, Y. Amini and M. A. Moosavian, A comprehensive study on the kinetics and isotherms of D_2/H_2 adsorptive separation using pure and composite Cu-BDC-NH_2 MOFs at 77 K, *Int. J. Hydrogen Energy*, 2024, **61**, 893-900.